Compensation of the Meyer-Neldel Compensation Law for H diffusion in minerals

Alan G. Jones[1]

[1]Geophysics, School of Cosmic Physics, Dublin Institute for Advanced Studies, Dublin, Ireland

Abstract The Meyer-Neldel Rule (MNR), or compensation law, linearly relates the preexponent term to the logarithm of the excitation enthalpy for any process that is thermally driven in an Arrhenian manner, and MNR fits can be used to calibrate and validate laboratory experimental results. Both robust least squares linear regressions and nonrobust regressions on selected subsets for individual minerals with sufficient experimental data demonstrate that hydrogen diffusion in minerals obeys the MNR with differing MNR intercepts and gradients depending on the mineral. In particular, nominally anhydrous mantle minerals have very distinct and different MNR parameters compared to hydrous and crustal minerals, with garnet proving to be an outlier lying in between the two. Furthermore, the variations of the estimated intercepts and gradients of the various MNRs are not random, but remarkably they themselves fall on a striking linear trend. This observation, if more broadly true, has profound implications for materials sciences and understanding of solid-state physics, as it implies that the compensation rule is itself compensated.

1. Introduction

The Arrhenius equation is a simple description of any process that is thermally activated, and is:

$$X = X_0 \exp\left(-E/kT\right), \tag{1}$$

where E is the activation energy of the process (in eV), k is Boltzmann's constant, X_0 is the preexponent term, and T is the temperature (in Kelvin) (alternatively, in some fields E is reported in kJ/mol and k is replaced by R, the gas constant). It was initially proposed in 1884 by Dutch physical chemist Jacobus Henricus van't Hoff to describe empirical observations of the temperature dependence of chemical reaction rates. Five years later, Swedish physical chemist Svante August Arrhenius, working with van't Hoff in Amsterdam after spending time with Ludwig Boltzmann in Graz, provided a theoretical justification for it based on his work on the disassociation of electrolytes [*Arrhenius*, 1889]. Equation (1) is as remarkably successful as it is simple, and finds application in many areas of science besides the obvious ones on reaction rates [e.g., *Hanggi et al.*, 1990], ranging from soil respiration [*Lloyd and Taylor*, 1994] to the growth rate of bacterial cultures [*Ratkowsky et al.*, 1982] to the drying of thin slices of garlic [*Madamba et al.*, 1996]. In the geosciences, its main applications describe electrical and thermal conduction in Earth materials, chemical denudation, geochemical process reactions, chemical weathering, diffusion processes [*Zhang et al.*, 2011], rheology, etc.

Initially in chemistry in the middle to late 1920s [*Constable*, 1925; *Cremer and Schwab*, 1929; *Schwab*, 1929; *Polissar*, 1930, 1932], then independently shortly later in physics [*Meyer and Neldel*, 1937], scientists began to observe empirically a linear relationship between the logarithm of the preexponent term X_0 and the activation energy E (more correctly activation enthalpy) for any process that could be described by an Arrhenius equation. Comparing the natural logarithm of X_0 with E, then a simple linear relation was found to hold for many materials and processes:

$$\ln\left(X_0\right) = a + b\,E, \tag{2}$$

where intercept a and slope b are constants. This rule, termed the Meyer-Neldel rule [*Meyer and Neldel*, 1937] (MNR) in physics and the compensation law or isokinetic relationship in chemistry [*Linert and Yelon*, 2013], (also in different guises the Barclay-Butler rule [*Barclay and Butler*, 1938], the θ rule [*Schwab*, 1950], the Smith-Topley effect [*Manche and Carroll*, 1979], and the Zawadzki-Bretsznajder rule [*Zawadzki and*

Bretsznajder, 1935]) is upheld in many areas of materials science in physics, chemistry, and biology, including compounds in semiconductors, various reduced oxide semiconductors, biological death rates, and chemical reactions [see *Yelon et al.*, 1992; also special volume of Monatshefte für Chemie, vol. 144, issues 1–2, edited by *Linert and Yelon*, 2013].

Substituting (2) into (1) yields:

$$\ln X = \ln X_0 + -E/kT = a + (b - 1/kT)\, E \, . \tag{3}$$

This implies that if the compensation law exists for a substance, the process converges to a constant characteristic value of *exp*(a) at the characteristic temperature $T_0 = 1/bk$, which is termed the isokinetic temperature and is a value particular to each process and each material.

Solid-state physicists have discussed the MNR for many years (see discussion in *Widenhorn et al.* [2002]), with *Dyre* [1986] proving that only one valid phenomenological model exists that explains it, and that model is based on an exponential probability distribution of energy barriers. Some have concluded that it is a consequence of a one phonon activated process [*Yelon et al.*, 1992, 2006], with the suggestion that minerals/species that have large activation barriers (large E) to diffusion compensate by increasing their attempts to diffuse [*Boisvert et al.*, 1995]. *Shimakawa and Aniya* [2013] recently presented a new model to explain the MNR in atomic diffusion of condensed matter taking into account phonon absorption and emission processes by diffusing atoms.

The MNR is not without contention however, even to the point of discussion on statistical significance of fitting experimental data [*Dunstan*, 1998; *Barrie*, 2012c, 2012a, 2012b; *Yelon et al.*, 2012]. Nevertheless, this empirically observed rule is being demonstrated to be upheld in more and more cases, and it can be employed to check laboratory observations and to provide fundamental constraints on the derivation and estimation of X_0 and E from experimental data given their interrelationship through the MNR. Thus, this relationship can be used to calibrate and validate laboratory experiments, an example is given in *Jones* [2014] for proton conduction in olivine, and indeed can be used to determine an appropriate value for one of them given the other, as shown for oxygen diffusion in diopside by *Jaoul and Bejina* [2005] for their geospeedometry calculations.

For diffusion generally, the MNR has been demonstrated to be upheld for a wide variety of diffusing species in a wide variety of materials [e.g., *Mehta*, 2010; *Shimakawa and Aniya*, 2013]. Indeed, *Boisvert et al.* [1995] make the bold statement that "we have unambiguously established the validity of the Meyer-Neldel law for phonon-activated Arrhenius processes" based on their consideration of diffusion on metallic surfaces. The impact of this confirmation and validation of the MNR has yet though to find its way into the geosciences in a meaningful manner.

For diffusion in minerals, numerous workers have shown that the MNR is upheld for many diffusing species in individual minerals, with the first study being that of *Hart* [1981]. Examples include oxygen diffusion in diopside [*Jaoul and Bejina*, 2005], in perovskite [*Berenov et al.*, 2001], and in a wide variety of minerals [*Zheng and Fu*, 1998], silicon diffusion in silicate minerals [*Bejina and Jaoul*, 1997], Fe, Mn, Mg, and Ca diffusion in garnets [*Korolyuk and Lepezin*, 2008] (where Fe, Mn, and Mg are fit as one diffusing species), argon diffusion in sericites [*Batyrmurzaev*, 2003], Fe/Mg interdiffusion in olivines and garnet [*Jaoul and Sautter*, 1999], and Ar, H, Pb, and Sr diffusion in a wide array of minerals [*Zhao and Zheng*, 2007]. Proton diffusion has been studied the most of all diffusing species, and adherence to the MNR has been reported for perovskites [*Kreuer*, 1999], as well as other crustal and upper mantle minerals discussed below. *Brady and Cherniak* [2010] give an excellent recent review, and discuss the consistency of the Arrhenius parameters with the MNR for He, Ar (hydrous silicates only), Mg, Pb, REEs, Si, Sr, Ca, and for the alkaline earth elements as a group. Na and K are reported to show less consistency, but explained as possibly due to the limited range of activation energies observed. Hydrogen diffusion is not treated extensively in their review, only that by excluding H, He, and Li values they obtained a very good linear fit for diffusion by the other species in diopside and plagioclase.

In this paper, we will closely examine the MNR relationships derived for hydrogen diffusion in different minerals in the Earth's crust and upper mantle. This examination is primarily not conducted on an experiment-by-experiment, case-by-case basis, but through employing modern robust statistical methods to perform

linear regressions after automatically removing outliers, identified objectively not subjectively, and assuming there is error in both fitted Arrhenius values (preexponent term and activation energy). In addition though, following more standard practice we consider subsets of data that have been subjectively selected, on objective grounds, for inclusion. We show that either approach yields the same MNR estimates, with the robust ones being statistically superior (smaller error estimates, larger correlation coefficients).

Furthermore, we show that the various MNR intercepts and gradients for the different minerals all themselves fall on a straight line, suggesting that the Meyer-Neldel Compensation Law is itself compensated. It needs to be tested whether this is a general result for processes that can be described by the Arrhenius equation, but if so then the implications for one phonon processes are profound.

2. MNR Parameters for Hydrogen Diffusion in Minerals

Herein, we consider diffusion in Earth minerals, specifically hydrogen diffusion for which the most extensive experimental observations exist, and take advantage of four recently compiled databases [*Ingrin and Blanchard*, 2006; *Zhao and Zheng*, 2007; *Brady and Cherniak*, 2010; *Farver*, 2010] plus prior work of others (see supporting information Table S1) and some newer data. (Where possible, original sources were checked; a few errors were found in the review compilations.)

There is an immense body of literature in the Solid-State Physics community, vastly larger than the geoscience community by an order of magnitude, reporting hydrogen diffusion in many materials, particularly those of interest to semiconductor and fuel cells research (e.g., silicon, germanium, palladium, lithium, etc.), but here we restrict ourselves to Earth's crustal and upper mantle minerals. We note that hydrogen has rapid diffusion rates compared to other species (hence its interest to the electromagnetic induction community since the insightful paper by *Karato* [1990]), demonstrating that hydrogen diffuses through the lattice as protons not coupled to other ionic species [*Farver*, 2010].

Supporting information Table S1 is a collation from all sources, mostly from review papers (with original references cited) but also original sources. Duplicate entries are noted and removed. If there are different model fits to the same raw diffusion data, these represent different and independent pairs for inclusion in the robust regression analysis; these different models are though excluded from the subjectively selected subsets. Table 1 is undoubtedly incomplete, likely contains errors and inconsistencies from the published sources and from transcription between the different units used by different authors, but it does represent the most complete ensemble of estimates of Arrhenius fits to hydrogen diffusion data published to date. The collection lists *effective diffusivity*, which is dominated by lattice (i.e., vacancy) diffusion but may contain results of interstitial diffusion. Also, at least one grain boundary diffusion point [*Demouchy*, 2010] is included on purpose in the robust regressions of olivine and sets containing olivine to test the statistical methods adopted for their ability to identify and cull incompatible points. Grain boundary diffusion is known to be far faster than lattice or interstitial diffusion [e.g., *Dohmen and Milke*, 2010], but are the Arrhenius values found consistent or inconsistent with the Arrhenius values of the other processes? This we test through consistency with, or lack thereof, the MNR regression. That grain boundary diffusion point is removed from all selected sets of data.

The primary approach taken here for analyzing the minerals data sets is an objective statistical one for identifying and removing outliers. An alternative approach is to examine each data pair of values (activation energy and preexponent coefficient) and decide whether the pair should be included in, or excluded from, further analysis based on knowledge of experimental procedures. Such a subjective approach may lend itself to the introduction of significant bias error though unwarranted exclusion of data or through lack of exclusion of other data as there may be insufficient information upon which to make an informed decision. Indeed, we *know* that the *Demouchy* [2010] point is a measurement of grain boundary diffusion in olivine—but what about those points resulting from experiments where the dominant diffusion process, lattice (vacancy), interstitial or grain boundary, is unknown? Robust statistical methods offer the objective tools to perform identification and rejection of outliers that do not conform to the general model. However, to demonstrate the similarities and possible differences between automatic statistical culling based on outlier identification and careful selection, the regressions on each mineral data set are performed twice, once with all data (excluding duplicate data) performing robust regressions using iterative culling, and the second time

Table 1. LS Regression Models of the Intercept (a) and Slope (a), With Their Standard Errors (SE), of Hydrogen Diffusion in Minerals Using a Robust Fasano-Vio LS Regression with Rousseeuw LTS With Cook's Distance Based Rejection Iterating Until the "Knee" of SE Descent Curve[a]

Data	Intercept (a) ($\log_{10}$ (D_0 (m^2/s)))	Gradient (b) ($\log_{10}$ (D_0 (m^2/s)/eV))	SE a ($\log_{10}$ (D_0 (m^2/s)))	SE b ($\log_{10}$ (D_0 (m^2/s)/eV))	Correlation Coefficient	Isokinetic Temperature (°C)
All (olivine (24), pyroxenes (15), rutile (13), other NAMs (2), garnet (12), quartz (11), feldspars (2), amphibole (5), hydrous minerals (53), 137 points total, 45 culled)	−11.2	4.03	0.26	0.15	0.94	1000 ± 50
All selected (olivine (15), pyroxenes (15), rutile (9), other NAMs (2), garnet (12), quartz (7), feldspars (2), 62 points selected)	*−11.6*	*−4.07*	*0.46*	*0.22*	*0.91*	
Mantle minerals—olivine (24), pyroxenes (15), rutile (13), other NAMs (2) (54 points, 4 culled)	−9.60	3.17	0.32	0.16	0.94	1300 ± 80
Mantle minerals (olivine (15), pyroxenes (15), rutile (9), other NAMs (2), 41 points selected)	*−9.98*	*−3.28*	*0.40*	*0.19*	*0.93*	
Crustal minerals—quartz (11), feldspars (2), amphibole (5) (18 points, 4 culled)	−18.4	8.49	0.77	0.53	0.98	320 ± 40
Crustal minerals (quartz (7), feldspars (2), 9 points selected)	*−17.8*	*−7.75*	*1.85*	*1.21*	*0.91*	
Olivine (24 points, 3 culled)	−8.89	2.67	0.45	0.22	0.94	1600 ± 150
Olivine (15 points selected)	*−9.06*	*2.71*	*0.59*	*0.26*	*0.90*	
Pyroxenes (15 points, 1 culled)	−10.4	3.49	0.88	0.40	0.92	1200 ± 160
Pyroxenes (15 points selected)	*−10.9*	*3.68*	*0.96*	*0.45*	*0.90*	
Pyroxenes monoclinic (11 points, 2 culled)	−10.2	3.24	0.79	0.36	0.96	1300 ± 175
Pyroxenes orthoclinic (4 points, 1 culled)	−14.7	4.86	0.83	0.35	0.99	765 ± 75
Rutile (13 points, 3 culled)	−8.81	3.25	0.36	0.37	0.95	1300 ± 180
Rutile (9 points selected)	*−10.9*	*4.67*	*1.19*	*1.13*	*0.77*	
Garnet (12 points, 2 culled)	−12.5	4.73	0.49	0.23	0.99	800 ± 50
Garnet (12 points selected)	*−11.9*	*4.28*	*0.65*	*0.28*	*0.98*	
Quartz (11 points, 2 culled)	−19.6	9.05	0.86	0.54	0.99	280 ± 35
Quartz (7 selected)	*−18.9*	*8.83*	*1.90*	*1.41*	*0.93*	
Amphibole (5 points, 2 culled)						
None selected	−23.8	14.2	0.96	0.96	0.99	82 ± 25
Hydrous minerals (53 points, 5 culled)	−17.0	7.56	0.87	0.84	0.67	400 ± 75
None selected						
MNR LS Regressions From Brady and Cherniak [2010]						
Alkali feldspars	−12.65	2.73			0.62	1575
Diopside	−20.04	3.68			0.97	1100
Plagioclase	−14.70	2.70			0.83	1600
Quartz—Li, Na, K, and Ca	−9.61	3.73			0.95	1080
Quartz—Si and Ti	−14.07	2.33			0.93	1890
MNR Regression for H Diffusion in All Minerals From Zhao and Zheng [2007]						
All minerals	−13.1	4.87	0.67	0.24	0.96	760 ± 7

[a]The second line for each individual mineral (in italics) and the sets represents the nonrobust FV LS regression for those data selected from the ensemble as being appropriate for inclusion based on consideration of experimental procedure.

using nonrobust regressions on only those points in each set considered appropriate through careful selection.

The diffusion equation for a single diffusing species is:

$$D = D_0 \exp\left(-E/RT\right), \tag{4}$$

where D is the diffusion rate (m^2/s), D_0 is the preexponent diffusion rate (m^2/s), E is activation enthalpy (J/mol), R is the gas constant (J/mol K), and T is the temperature (K). Others have previously considered the MNR applied to diffusion, initiating with the work by *Winchell* [1969] on silicate glasses, then more generally for natural silicate minerals in the compilation and analysis by *Hart* [1981]. A broad treatment of diffusion by many species in many minerals is contained in the recent review by *Brady and Cherniak* [2010]. Two prior MNR analyses considered diffusion of individual species in all minerals simultaneously [*Zhao and Zheng*, 2007] and the diffusion of all species, except hydrogen, simultaneously in individual minerals [*Brady and Cherniak*, 2010], but this is the first study to consider all available data for a single species of diffusion, namely hydrogen, in many minerals separately, and to demonstrate a rather remarkable phenomenon.

The Arrhenius least squares model fits reported in the literature for the minerals considered are listed in Table 1, and are olivine (24 values), pyroxenes (17 values), and rutile (13 values), other NAMs (2 values), grouped in the "mantle" group, garnet (12 values) in its own group, then quartz (12 values), feldspars (2 values), and amphiboles (5 values) in the "crustal" group, finally hydrous sheet and other silicates (56 values).

The robust least squares (LS) regressions were performed using Rousseeuw's Least Trimmed Squares (LTS) [*Rousseeuw*, 1984] approach with Cook's Distance [*Cook*, 1977] based rejection, iterating to the "knee" of the standard error descent curve, analogous to the L-curve approach in nonlinear inversion [*Hansen*, 1992], assuming error on both the activation enthalpy and the preexponent component using Fasano and Vio's (FV) [*Fasano and Vio*, 1988] adaptation of York's [*York*, 1966] method (see description and example application in the supporting information for more details). At the knee the estimates of intercept and slope and their associated errors are such that succeeding culling iterations yield estimates that lie within the errors of the estimates at the knee point. There is no justification for continuing with further culling iterations beyond this point. In addition, the data sets have been multiply refined and reduced by excluding or including points to test for bias and for contamination, and the combinations tested all resulted in the same final MNR parameters, to within statistical estimation error. As we will show, for only one set of data do the robust regression estimates differ significantly, i.e., more than one standard deviation, from the regression estimates made on selected data.

2.1. Regression to Olivine Diffusion Data

As an example of the regression approach, the experimentally determined values of E (in eV rather than kJ/mol, where 1 eV = 96.4869 kJ/mol, for consistency with MNR results for diffusion as reported in the solid-state physics literature and in other geoscience subdisciplines, such as electrical conduction in minerals) and $\log_{10}(D_0)$ (base-10 logarithm rather than natural logarithm, with D_0 in m^2/s) for diffusion of hydrogen in olivine are plotted in Figure 1, totaling 24 separate estimates, including two very recent well-calibrated values by *Padrón-Navarta et al.* [2014] (the two red points with error bars). A standard least squares (LS) regression to these 24 values, as performed with, e.g., Excel and most other off-the-shelf codes, yields an intercept and slope of (-8.17 ± 0.62, 2.26 ± 0.31) (red line in Figure 1) with a correlation coefficient of 0.84. However, a standard LS regression assumes that the X data along the ordinate are independent, i.e., without error, which is a fallacy in this case (and in many other cases in the sciences), and that there are no outliers in the data set; outliers cause severe leverage effects and result in hugely erroneous regression estimates. The
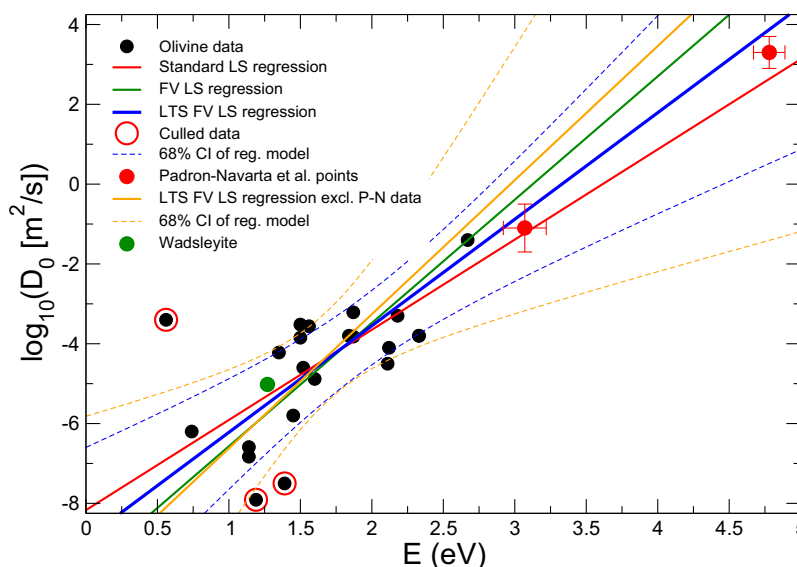
Figure 1. Plot of Arrhenius parameters from 24 data values for hydrogen diffusion in olivine with least squares (LS) regression fits to the points. The standard least-squares regression is shown by the red line, the Fasano-Vio (FV LS) regression by the green line, and the least trimmed squares robust Fasano-Vio (LTS FV LS) regression by the blue line after culling the three data points outlined with red circles. Dashed blue lines are the 68% confidence intervals on the LTS FV LS regression. The orange line, with its 68% confidence limits (dashed orange lines), is the regression excluding the *Padrón-Navarta et al.* [2014] data shown in red.
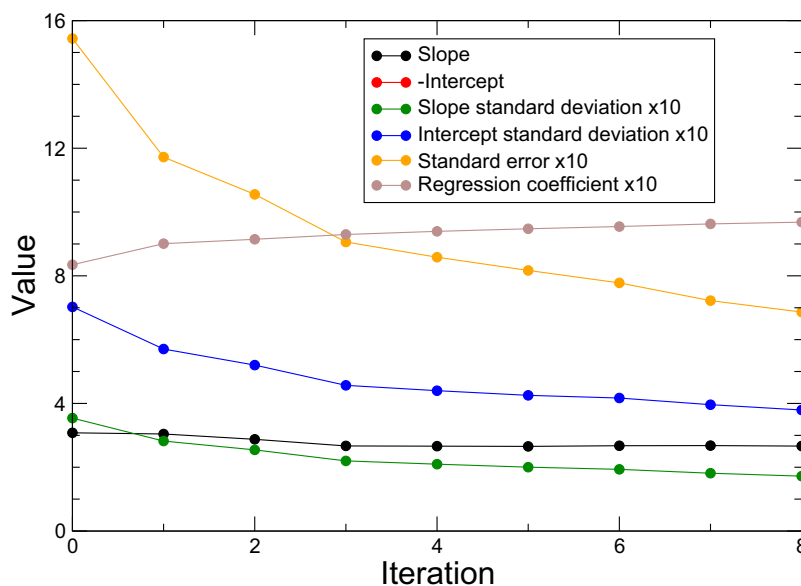
Figure 2. Variation of MNR slope and intercept, and their errors and the regression coefficient, with increasing iteration of the robust Fasano-Vio LTS regression for the olivine diffusion data shown in Figure 1.

Fasano-Vio (FV) LS regression to all 24 data points yields different intercept and slope of (-9.66 ± 0.71, 3.09 ± 0.36), with a correlation coefficient also of 0.84 (green line in Figure 1).

Applying the LTS FV robust scheme to the 24 points yields the variations of the slope, intercept, and their standard errors and correlation coefficient with delete-1 culling iterations as shown in Figure 2, where the knee of the standard deviation and the asymptotic behavior of the slope and intercept suggest that three points need to be removed. The FV LS regression when those three points are removed has an intercept and slope of (-8.89 ± 0.45, 2.67 ± 0.22) (blue line in Figure 1) and a far higher correlation coefficient of 0.94. Figure 3a shows the intercept and slope pairs for each iteration, together with their error estimates, and after three iterations the solution converges with estimates from further iterations remaining within the error bounds of those from the third iteration. Figure 3b shows the individual delete-1 estimates for each culling iteration, and the clustering for iteration 3 and higher iterations demonstrates the insensitivity of the MNR estimates to individual data pairs from the data set once the three outliers have been culled.

The culled points are identified in Figure 1 and are indicated in supporting information Table S1 in the order of being culled (C1, C2, and C3). One point is an obvious outlier, and that is the olivine value at ($E = 0.56$ eV, $\log_{10}(D_0) = -3.4$) that was reported by *Demouchy* [2010, 2012] for grain boundary diffusion. Grain boundary diffusion is an entirely different process from lattice diffusion, so it is not surprising that this point is discordant with the rest of the olivine diffusion data set. This point was the first to be culled by the LTS FV LS algorithm in any of the sets that included it, further demonstrating the veracity of the LTS approach at identifying outliers that are inconsistent with the bulk of the data set. The point was included purposely to test the efficiency of the approach at recognizing and culling outliers, and the scheme performed flawlessly regardless of the subset analyzed. The second point to be culled is that derived from *Libowitzky and Beran* [1995] of (1.39, -7.50) reported in the compilation of *Ingrin and Blanchard* [2006], and the third is that of (1.19, -7.91) derived by *Zhao and Zheng* [2007] using an ionic porosity law.

Another important point to be gleaned from Figure 3b is that any subjectively chosen subset of the olivine data set of 24 points will result in LS regression MNR estimates within statistical errors of those listed in Table 1 for olivine, provided that the same three points are removed as identified objectively by the LTS culling iterations. Although the inconsistency of the *Demouchy* [2010, 2012] point is obvious, the danger inherent in subjective selection is in not identifying the consequences of including the two other points, (1.39, -7.50) and (1.19, -7.91).

Note that the single model Arrhenius data for wadsleyite of (1.27, -5.02) (green point in Figure 1) in the *Brady and Cherniak* [2010] collation lies almost on the regression model line for olivine, and well within the
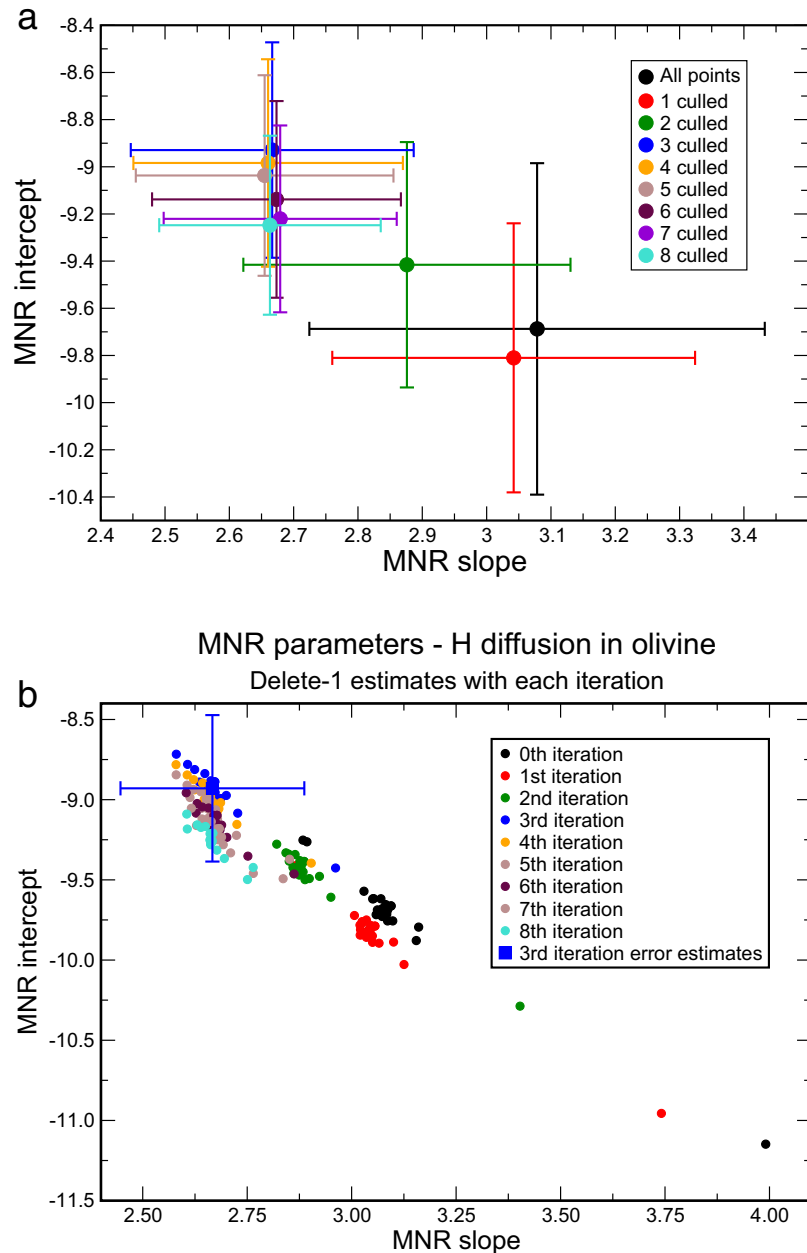
Figure 3. Variation of MNR slope and intercept with increasing iteration of the robust LTS Fasano-Vio LS regression for the olivine diffusion data shown in Figure 1. (a) Estimates of the MNR parameters with error for each culling iteration. (b) DeleteS estimates of the MNR parameters for each iteration.

one sigma confidence intervals of the regression. Its exclusion has no effect on the LTS FV LS regression— almost exactly the same model is returned (-8.95 ± 0.47, 2.69 ± 0.23) without it compared to (-8.89 ± 0.45, 2.67 ± 0.22) with its inclusion, both with a correlation coefficient of 0.935. It is surprising that diffusion of hydrogen in the high pressure form of olivine should fall exactly on the MNR line for olivine itself, given that wadsleyite has a very different lattice structure from olivine. This calls for further examination and understanding of hydrogen diffusion in higher pressure phases.

A second regression was performed on the selection of 15 values from this data set of 24 chosen for their appropriateness based on experimental procedure; the reason for removal of those rejected, marked with an X, is given in Table 1. The nonrobust FV LS regression to those 15 points yields an MNR model of (-9.06 ± 0.59, 2.71 ± 0.26) with a correlation coefficient of 0.90. This model lies well within the LTS FV LS

model of (-8.89 ± 0.45, 2.67 ± 0.22). This selection, although it is based on objective criteria is nonetheless a subjective one; other workers may have included some of the discarded data or excluded others. However, as shown by the clustering in Figure 3b, it is immaterial which data are selected; provided the three points identified by the robust regression are removed, a statistically consistent regression model will result.

The two Arrhenius model pairs of *Padrón-Navarta et al.* [2014] for olivine, (3.07, -1.1) and (4.78, 3.3) (red points in Figure 1), were published as this paper was in second revision and are particularly worthy of more detailed examination. These two are very interesting as they are estimates of different rates of diffusion of hydrogen from different substitution sites within the lattice. The fastest diffusion rates were observed for hydrous defects related to trivalent cations and Mg vacancies in the Ti-doped forsterite, with slower diffusion by the hydrous defects related to Ti and a fraction of the hydrated Si-vacancies. Far slower was the diffusion of hydrogen from Si-vacancies in the undoped MgO-buffered experiments. The nonrobust standard LS fits to the data yielded Arrhenius pairs of (3.07 ± 0.15, -1.1 ± 0.6) (i.e., activation enthalpy of 296 ± 14 kJ/mol with a preexponent D_0 of $10^{-1.1 \pm 0.6}$) for [Si] and [Ti] in the Ti-doped fosterite, and (4.78 ± 0.11, 3.3 ± 0.4) (461 ± 11 kJ/mol with a preexponent D_0 of $10^{3.3 \pm 0.4}$) for [Si] in the undoped MgO-buffered fosterite. As is often the case with such regression model fits, the gradient, i.e., the activation enthalpy, is better resolved with lower error than the intercept, i.e., the preexponent component.

The original version of this manuscript only considered the 22 model diffusion in olivine estimates without the two new data of *Padrón-Navarta et al.* [2014]. The LTS FV LS regression to those 22 data pairs, with the same three points culled, yields a model with an MNR intercept and slope of (-9.98 ± 0.87, 3.36 ± 0.50), with a correlation coefficient of 0.79 (orange line in Figure 1 with 68% confidence intervals shown). This model lies, within error, statistically close to the model including those two points, i.e., (-8.89 ± 0.45, 2.67 ± 0.22).

A test of how well this MNR approach is performing is to examine the prediction of the Arrhenius preexponent component given the activation enthalpy, or of the activation enthalpy given the preexponent component, for those two new data based on the prior regression model. However, as is obvious from Figure 1, the two new points have activation enthalpies that are outside to well outside those previously reported for hydrogen diffusion in olivine, and the extrapolation to those higher values is with very poor confidence, as signified by the 68% confidence intervals of the prior model (orange dashed lines in Figure 1). This will be explored further below with the mantle data set, as it contains activation enthalpies that overlap with the two new points.

2.2. Regressions to All Other Individual Minerals

The experimentally determined values of E and $\log_{10}(D_0)$ for all minerals are listed in supporting information Table S1 and are plotted in Figure 4, together with best-fitting robust linear regressions to all of the data and various subsets, following the approach described above for olivine. The LTS FV LS regressions to the data sets and subsets are listed in Table 1. For all individual sets of minerals, only a small fraction of the data, up to three points at most, needed to be culled to obtain stable regressions. The amphibole set comprises only five points, and two of them are culled to yield a stable regression. Thus, the regression is only to three points, and hence the amphibole MNR estimates are not used in the regression to the individual minerals below.

For the very heterogeneous "all data" set far more need to be culled, 45 points of the 137 data, which is evidence that the set cannot validly be described by a single regression. This is discussed further below.

Nonrobust regressions are performed of selected data in each mineral set, and of the combinations of the mineral sets. The parameter estimates and their errors are given in Table 1 in italics. Note that in all cases, except for rutile, the nonrobust regressions of the selected data are exactly the same, to within error bounds, of the robust estimates on nonselected data, with the robust estimates having superior statistics (smaller error estimates, larger correlation coefficients). This demonstrates that objective culling using robust statistics is as effective at determining the MNR parameters as subjective selection made by experts in diffusion.

Note that all hydrous minerals are rejected for subjective analysis (amphibole, hydroxyl minerals) as OH- and H_2O are major elements in those minerals and not trace elements as in nominally anhydrous minerals (NAMs). Major elements are known to have concentration-dependent diffusivity, as for example an Fe-Mg interdiffusion coefficient. This likely explains the much broader field for the hydrous minerals compared to NAMs. Nonetheless, the LTS FV LS regression yields MNR estimates for the slope and intercept of the
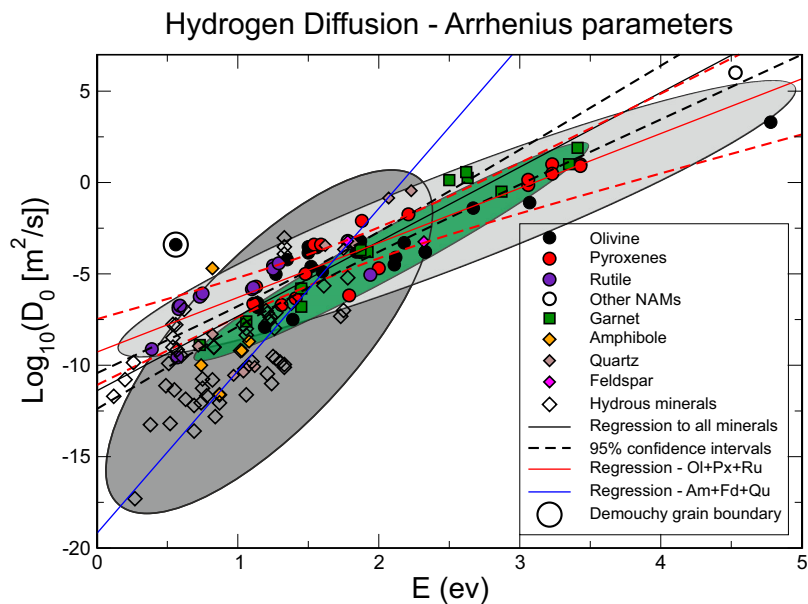
Figure 4. Plot of Arrhenius parameters for hydrogen diffusion in minerals. Mantle minerals shown in circles, crustal minerals in diamonds. LS regressions to all data (solid black line with 95% confidence intervals) and crustal (Am + Fd + Qz) and mantle (Ol + Px + Ru) subsets shown. The two gray fields encompass the mantle and NAM minerals (light gray) and crustal and hydrous minerals (dark gray) fields, respectively, and the green field encompasses the garnet data. The double circle is the olivine data point of *Demouchy* [2010, 2012] for grain boundary diffusion.

hydrous mineral set that are well within 1σ of the MNR estimates for the selected crustal minerals set, so are statistically indistinguishable.

Also listed in Table 1 for comparison and completeness are the regression models derived by *Brady and Cherniak* [2010] for diffusion by all species, excluding hydrogen, in specific minerals, and that of *Zhao and Zheng* [2007] for hydrogen diffusion in all minerals taken together. Given the variation that exists in MNR parameters for different diffusing species and for different minerals, such averaging is questionable. The *Brady and Cherniak* [2010] data are included here to emphasize the point that diffusion of one species in a material will not necessarily yield the same MNR parameters as other diffusing species, and unless proven otherwise, all diffusing species should be considered independently. The exercise performed here for hydrogen must be performed for each other diffusing species individually in each mineral.

There are essentially two sets of MNR parameters—a set comprising nominally anhydrous dominantly mantle minerals (NAMs, light gray field in Figure 4) that has a shallow MNR gradient (3.25–3.5), and a set comprising crustal minerals and dominantly crustal hydrous minerals (dark grey field in Figure 4) that has a far steeper gradient (9.0–10.0), with garnet lying in between the two (gradient of 4.0) (green field in Figure 4). The isokinetic temperatures for hydrogen diffusion in the specific minerals are listed in Table 1 and for the subsets is of the order of midcrustal temperatures (approximately 300–400°C) for crustal minerals and deep lithospheric to asthenospheric temperatures (1200–1600°C) for mantle minerals, with garnet at midlithospheric temperatures (800°C).

The mantle minerals are all (nominally) anhydrous, whereas the crustal minerals comprise hydrous and anhydrous (quartz, feldspar) minerals. Garnet is anomalous and lies between the two sets. Dividing the garnet set into crustal (grossulars) and mantle (pyrope) subsets does not make a difference, as the two arrays overlap each other and the estimates of the intercepts and slopes from the two LTS FV LS regressions lie within each other's error bounds.

2.3. Regression to All Data

Performing the LTS FV LS regression on the total data set of 137 points results in 45 being culled in order to get to the knee of the trade-off curve. The variation of the MNR slope and intercept for 59 culling iterations is shown in Figure 5, where the 0th iteration, i.e., all points regressed, is the pair on the bottom right of the
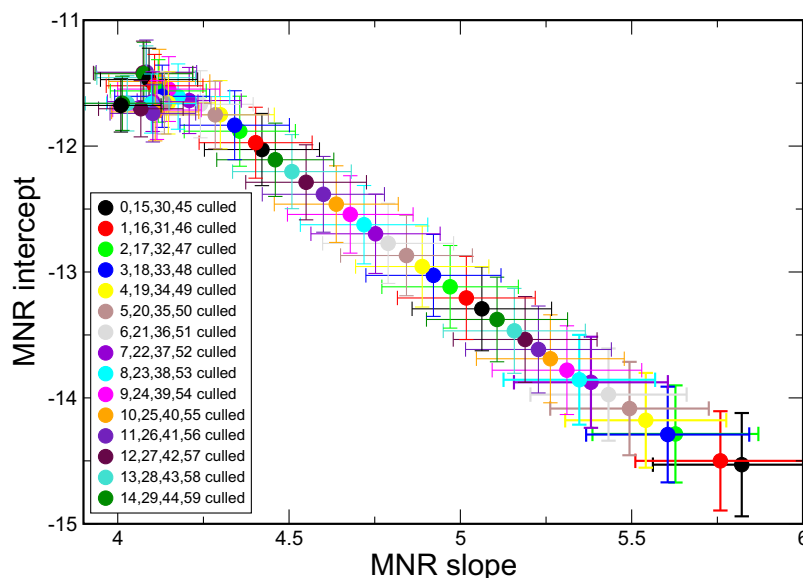
Figure 5. Variation of MNR slope and intercept with increasing iteration of the robust Fasano-Vio LTS regression for all 142 diffusion data shown in Figure 4.

plot, point (-14.5, 5.82) in black. Subsequent iterations moved the slope/intercept solutions progressively toward the top left, and after 45 iterations the solutions converged on asymptotic values of (-11.2, 4.03) for the intercept and the slope, respectively. The Arrhenius values being culled are all those lying in the bottom left side of Figure 4, i.e., all of the hydroxyl points, so it is not surprising that the All Data set has an MNR intercept and slope close to that for the mantle minerals.

This exercise highlights a caution when performing linear regressions; one must be careful that there are not two (or more) distinct processes operating that, due to the paucity of data and/or data error, are missed and the data are fit to a single process by adopting a linear regression. This effect is considered below in a detailed examination of the pyroxene data set.

2.4. Regression to Mantle Minerals

The model data for mantle minerals form a set that comprises 54 data; 24 for olivine, 15 for pyroxenes, 13 for rutile, and 2 for other NAMs (light gray set in Figure 4). Performing the same LTS FV LS regression approach as above yields a robust solution, after culling four data pairs, with an intercept and gradient of (-9.60 ± 0.32, 3.17 ± 0.16) with a correlation coefficient of 0.94 (orange line in Figures 4, and blue line in Figure 6).

The submitted version of this manuscript only considered 52 model diffusion estimates for mantle minerals, i.e., without the two new model olivine data of *Padrón-Navarta et al.* [2014], (3.07, -1.1) and (4.78, 3.3), and the LTS FV LS regression to those 52 data pairs, with four points culled, yielded a model with an MNR intercept and slope of (-9.90 ± 0.34, 3.40 ± 0.19), with a correlation coefficient of 0.93 (red line in Figure 6). This model lies within the error bounds of the model including those two points given above.

A test of how well this MNR approach is performing is to examine the prediction of the Arrhenius preexponent component given the activation enthalpy. For activation enthalpies of 3.07 and 4.78, then the regression without the two values, i.e., (-9.90 ± 0.34, 3.40 ± 0.19), yields a prediction of the base-10 logarithms of the preexponent components of 0.59 ± 0.92 and 6.53 ± 1.83, respectively, compared to the experimentally derived (nonrobust) results of -1.1 ± 0.6 and 3.3 ± 0.4, respectively. Both of these prediction estimates lie less than two sigma error estimates away from the derived values. The quality of future statistical predictions will improve as more data are analyzed and added to the ensemble.

3. Individual MNR Intercepts and Slopes

When the MNR regression models for the six individual mineral groupings for which sufficient experimental data exist (olivine, pyroxenes, rutile, garnet, quartz, and hydrous minerals; amphibole excluded as only three
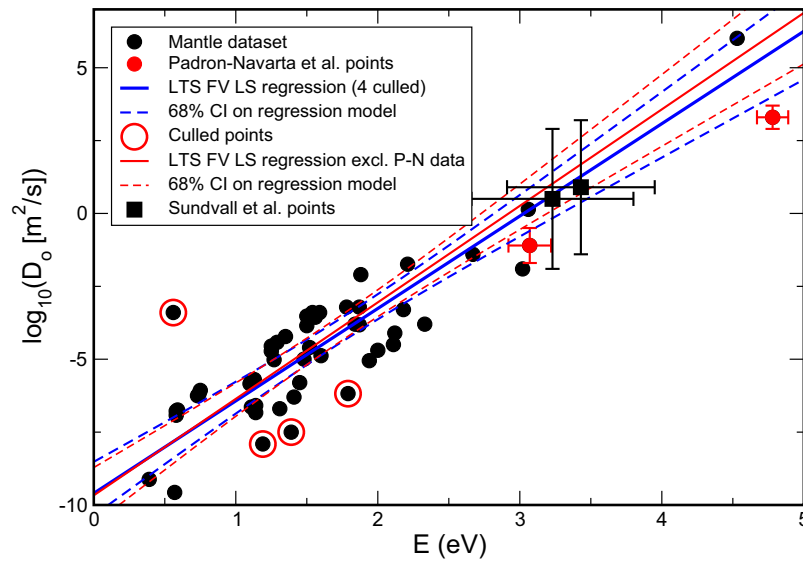
Figure 6. Plot of Arrhenius parameters from 54 data values for hydrogen diffusion in mantle minerals with the least trimmed squares robust Fasano-Vio (LTS FV LS) regression shown by the blue line after culling the four data points outlined with red circles. Dashed blue lines are the 68% confidence intervals on the LTS FV LS regression. The red points are the two new values of *Padrón-Navarta et al.* [2014]. The red line is the LTS FV LS regression to the data set excluding those points, i.e., 52 data, with 68% confidence intervals as shown. The data with black error bars are those of *Sundvall et al.* [2009] discussed in the text.

points fit by the regression) are plotted on a slope-intercept diagram, they are not random, but remarkably fall on a linear array (Figure 6) of the form:

$$a = \alpha + \beta b, \tag{5}$$

where a and b are the MNR intercept and gradient of equation (2). Not only do the individual minerals fall on a line, but also sets and subsets do as well, including the MNR estimates of *Zhao and Zheng* [2007] for hydrogen diffusion in all minerals. Note that the MNR estimates of *Brady and Cherniak* [2010] do not fall on this regression line, as those authors considered diffusion of all species except hydrogen in single minerals so the departure of their MNR values is not surprising. Those *Brady and Cherniak* [2010] points are included to firmly establish the argument that one cannot aggregate all diffusing species nor can one aggregate diffusion of one species in all minerals but must consider the diffusing species and minerals all independently.

Fitting the six MNR data for the individual mineral sets (olivine, pyroxenes, rutile, garnet, quartz, and hydrous minerals), listed in Table 1 and shown in Figure 7 with a (nonrobust) weighted Fasano-Vio regression yields:

$$a = -4.02\,(\pm 0.50) - 1.73\,(\pm 0.09)\,b$$

(on a log-10 scale rather than a natural logarithm scale), with a very high correlation coefficient of -0.995. Thus, for hydrogen diffusion in all minerals:

$$\alpha = -9.26\,(\pm 1.2)\,eV^{-1}\ and\ \beta = -3.98\,(\pm 0.21)\,eV^{-1}.$$

This is a remarkable—and totally unexpected—result. The six mineral sets were all analyzed and regressed independently to derive their MNR intercepts and slope. Yet when all six are plotted they fall on a linear array with an astonishingly high correlation coefficient of 0.98.

Note that the amphibole point, although not included in the regression, falls only 2σ away from the regression line.
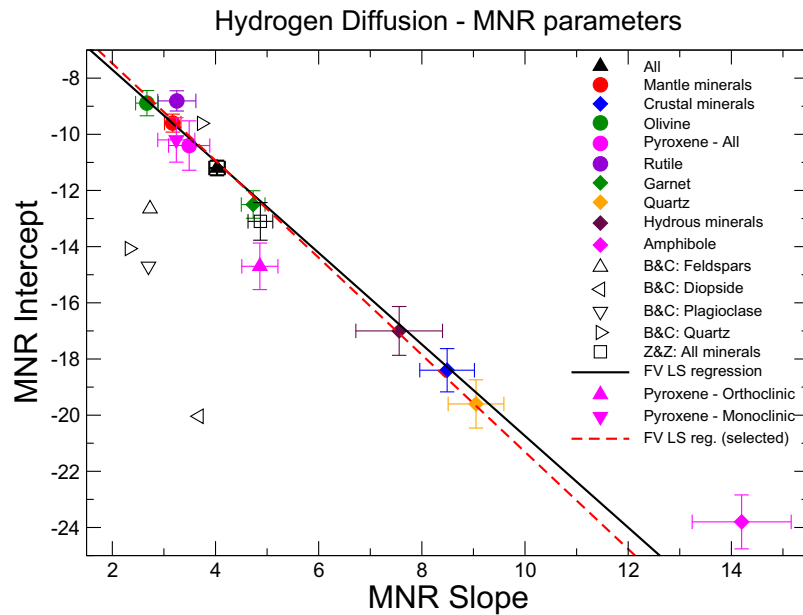
Figure 7. MNR intercepts and gradients for the LS regressions of hydrogen diffusion in individual minerals and subsets listed in Table 1 and shown in Figure 1, plus a regression through the six sets (black line) and a regression through the five sets of selected data (red dashed line). Also shown are the MNR parameters derived by *Brady and Cherniak* [2010] for diffusion by all species in specific minerals (open triangles), and of *Zhao and Zheng* [2007] for hydrogen diffusion MNR fit to all minerals (open square).

Performing a regression on the MNR models from five mineral sets that comprise selected data (olivine, pyroxenes, rutile, garnet, and quartz; MNR estimates in italics in Table 1) yields an FV regression model of:

$$a = -4.44 \, (\pm 0.84) - 1.63 \, (\pm 0.17) \, b$$

with a correlation coefficient of -0.984 (red dashed line, Figure 7). This model lies well within the regression model for the robust MNR parameters. For these five data, one must be wary of the regression as the quartz point (-18.9, 8.83) potentially acts as a leverage point and may have an unduly large influence on the regression estimates. However, an LTS FV LS regression culls instead the rutile value and the remaining four points yield a model of

$$a = -4.96 \, (\pm 0.23) - 1.59 \, (\pm 0.04) \, b$$

with a correlation coefficient of -0.999, which is statistically the same as the prior model.

4. Discussion

Arrhenius parameters for hydrogen diffusion in Earth's crustal and upper mantle minerals exhibit strong adherence to the Meyer-Neldel Rule (MNR), but with different MNR intercepts and gradients for each mineral. That they do this provides a powerful tool for assessing consistency between the derived activation energy and preexponent component and aids identification of outliers.

One example of application of the MNR is to refine the error associated with the preexponent D_0. The Arrhenius estimates along two crystallographic axes for the diopside sample studied by *Sundvall et al.* [2009] have activation energies of -331 ± 50 kJ/mol (-3.43 ± 0.52 eV, [010] axis) and -312 ± 55 kJ/mol (-3.23 ± 0.57 eV, [100] axis), and preexponents of $D_0 = 10^{0.9 \pm 2.3}$ m^2/s ([010]) and $10^{0.5 \pm 2.4}$ m^2/s ([100]). The points are shown in Figure 6 (black points with error bars) and in Figure 8 (red points with error bars), and the errors lie within the 68% confidence bounds (black dashed lines) of the linear regression (black line) so are compatible. For the pyroxene data, the confidence bounds are wide as there are so few data. If all mantle data are considered however (Figure 6), then the errors on the Arrhenius estimates of *Sundvall et al.* [2009] (black points with error
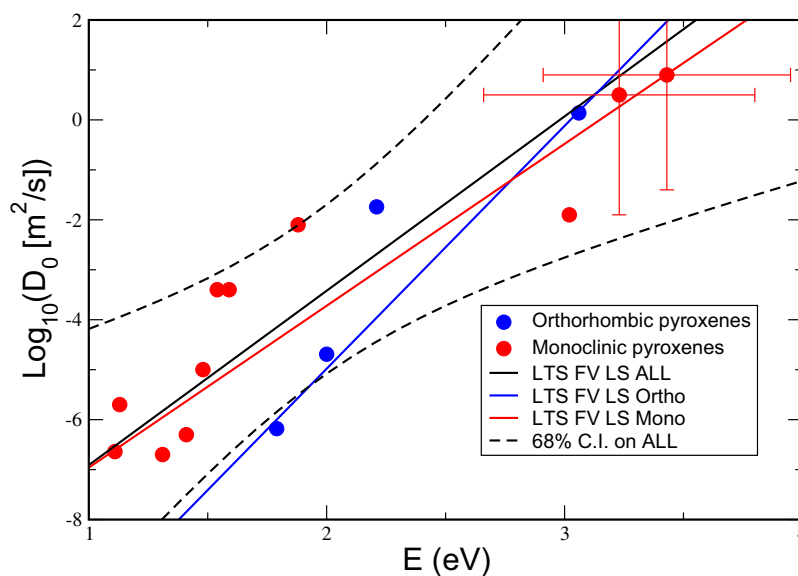
Figure 8. Regressions on pyroxene sets. Black line: All 15 points; blue points and line: four orthorhombic crystal points; red points and line: 11 monoclinic points. Black dashed lines are the 68% confidence intervals on the linear regression of all 15 data. The data with error bars are those of *Sundvall et al.* [2009].

bars) are clearly far too large given the 68% confidence bounds. The 68% confidence bounds for those points on the preexponent are $D_0 = 10^{0.9 \pm 1.0}$ m^2/s ([010]) and $10^{0.5 \pm 0.9}$ m^2/s ([100]).

There are statistically two groups of MNR intercepts and gradients for the bulk of the minerals studied, with garnet being an outlier not belonging to either set. One set comprises nominally anhydrous minerals (NAMs) from the upper mantle, and the other set comprises hydrous and crustal minerals. Why should there be two main sets of MNR intercepts and gradients?

One consideration could be the hydrous and anhydrous state of the minerals, with anhydrous minerals falling in the "mantle" cluster and hydrous minerals falling in the "crust" cluster. In support of this conjecture, *Lubianiker and Balberg* [1997] observed two Meyer-Neldel rules for DC conduction in porous silicon for the same temperature range, attributing one to extended-states transport and the other to thermally activated hopping. The former resembles that found in hydrogenated amorphous silicon, so the conduction is dominantly ionic transport, whereas for the latter conduction is by electronic transport.

An alternative possible insight comes from consideration of the experimental results of proton conduction in lanthanum ortho-niobate (LaNbO$_4$) by *Solis and Serra* [2011]. Proton conduction in a material is directly relation to hydrogen diffusion in that material through the Nernst-Einstein equation; it was consideration of hydrogen diffusion rates in mantle materials that led *Karato* [1990] to suggest a quarter of a century ago that observations of enhanced electrical conductivity in the mantle may be due to proton conduction. (The very difficult experiments have been performed by various laboratories since the mid-2000s, and, although there is significant disagreement between the laboratories [see *Jones et al.*, 2012 for a discussion of the various observations], all are consistent in showing that proton conduction is highly significant and increases electrical conductivity by orders of magnitude.) *Solis and Serra* [2011] showed that lanthanum ortho-niobate has two distinct MNR intercepts and gradients, a low temperature pair and a high temperature pair, and that the two temperature ranges correspond to two different crystal structures. At low temperatures below 550°C, lanthanum ortho-niobate is in a monoclinic (fergusonite-type) phase, whereas at high temperatures above 550°C, lanthanum ortho-niobate is in a tetragonal (scheelite-type) phase.

We note that for the mantle minerals, minerals in the olivine group crystallize in the orthorhombic system, pyroxenes are both orthorhombic (enstatite, orthopyroxene) and monoclinic (clinopyroxene, diopside), and rutile has a tetragonal unit cell. For the crustal minerals, quartz has a triagonal crystal structure, feldspars are monoclinic or triclinic, and amphibole can be monoclinic and orthorhombic. Garnets are most often found in the dodecahedral crystal habit. Thus, if crystal structure is significant, then the pyroxenes should

JONES   13

fall into two separate sets, one for the orthorhombic set (four values, blue points in Figure 8) and another for the monoclinic set (11 values, red points in Figure 8).

LTS FV regression models of the two individual pyroxene sets (orthorhombic and monoclinic, identified in supporting information Table S1) and the combined set are listed in Table 1 and are shown in Figure 8. For the orthorhombic set, one point is culled (2.21, −1.74) and the other three fit a line with MNR intercept and slope of −14.7 ± 0.83 and 4.86 ± 0.35, respectively, with an excellent correlation coefficient of 0.997. For the monoclinic set, two points are culled and the best-fit FV regression to the remaining nine data has an intercept and slope of −10.2 ± 10.79 and 3.24 ± 0.61, respectively, with a slightly lower correlation coefficient of 0.955. These two models are shown in Figure 7 (upward and downward pointing magenta triangles) and are distinctly different from each other with a two sample t statistic of 9.8, implying that one can reject the hypothesis that they come from the same process at greater than a 99% level of confidence. Note that the MNR slope and intercept for the monoclinic set (diopside) falls within the bounds of the other mantle minerals (Figure 6), whereas for the orthorhombic set (enstatite, orthopyroxene) the slope and intercept are closer to that for garnet (Figure 6). However, one should be very circumspect accepting this latter result, given the very small sample of only three points fit for the orthorhombic set.

5. Conclusions

There is no doubt that the Meyer-Neldel compensation rule (MNR) is not universally accepted, with arguably its biggest objection being the lack of an agreed physical explanation of the phenomenon. However, more and more cases are being reported in the Solid-State Physics community of diffusion by different species in different materials adhering to the MNR. In the geosciences the MNR is not well known, and even less utilized, and one purpose of this paper is to demonstrate its applicability.

The MNR is a powerful tool for calibrating and verifying determinations of the Arrhenius preexponent term and activation energy term fitting experimental data. As stated by *Brady and Cherniak* [2010] in their examination of adherence to the MNR by diffusion of various species in various minerals: "However, the use of compensation relations to help identify "outliers" or unusual," and therefore suspect (or very interesting!), diffusion data is quite reasonable". We agree with that position, and have employed statistical methods to identify the outliers. As an exemplar of this, we purposely included the grain boundary diffusion point of *Demouchy* [2010] in the olivine database, and found that it was always the first point to be culled by the LTS FV LS regression, regardless of the subset of olivine data that was chosen.

The MNR has been demonstrated to be valid for diffusion in minerals by other authors previously, but here we examine each mineral independently for only hydrogen diffusion, and derive statistically robust estimates of their distinct MNR gradients and intercepts based on the available data sets for each individual crustal and upper mantle mineral. The data analyzed, listed in supporting information Table S1, are *effective diffusivities* and are considered to be primarily reporting lattice diffusion rather than interstitial diffusion. However, if there is a mixing of the two, then given that so few data are culled in the LTS FV LS regression iterations, this would suggest that lattice and interstitial diffusion of hydrogen have the same MNR slopes and intercepts for each mineral. This may not hold for all diffusing species.

We also undertook nonrobust regressions of data that were carefully selected. The selection process, while based on objective grounds, is nevertheless subjective and is prone to user bias; some people will include different data and exclude others. However, satisfyingly the objective robust regression estimates are the same, to within error, as those determined from nonrobust culling regression of the selected data, with the sole exception of rutile.

We show unequivocally that for the minerals studied they fall into two clusters and one anomalous outlier, namely garnet. The clusters are of olivine, pyroxene, rutile, and other NAMs, in what is termed herein the "mantle group," and quartz, feldspar, amphibole, and hydroxyl silicates in the "crustal group." The isokinetic temperatures of the mantle group is of the order of that at the base of the lithosphere and the asthenosphere, around 1200–1600°C, whereas for the crustal group it is at a temperature commonly found in the midcrust, around 300–400°C. The isokinetic temperature for garnet lies in the midlithosphere at around 800°C.

The reason for the two distinct clusters could be due to whether the mineral is hydrous or anhydrous. Alternatively, the crystal lattice structure could be significant. Pyroxenes can be statistically divided into two

subgroups, one for orthorhombic lattice, namely enstatite and orthopyroxene, and the other for monoclinic lattice, diopside. The two subgroups display distinctly different Arrhenius parameters, but the sample sizes of the sets are small, particularly for the orthorhombic set (only three points!), and far more data need to be acquired to substantiate, or reject, this conclusion.

Most strikingly, when these individual MNR gradients and intercepts are plotted for the six minerals studied, they themselves fall on a straight line, with the intercept and gradient of the MNR parameters being $\alpha = -9.26\ (\pm 1.2)\ eV^{-1}$ and $\beta = -3.98\ (\pm 0.21)\ eV^{-1}$. The correlation coefficient for that regression is an astonishingly high 0.98. This cannot be a coincidence or due to inappropriate data analyses. One can discuss and debate the merits of including or excluding some of the data in the individual analyses, but as exemplified by Figure 3b such discussion is secondary in that the ensemble MNR estimates are robust, and the overarching result shown here is that these robust MNR estimates themselves fall on a linear array. This was confirmed through regression of the user-defined selected data sets.

The implication of this result is the generalization of the MNR: for a single diffusing species in a single mineral, those samples that have large activation barriers (large E) to diffusion compensate by increasing their attempts to diffuse (large preexponent). For a single diffusing species in all minerals, as in the case of hydrogen studied here, those minerals that have large average activation barriers compensate equally with increased diffusion attempts. Thus, the compensation rule is itself compensated.

Whether this phenomenon is observed for other Arrhenian processes needs to be tested.

References

Arrhenius, S. Z. (1889), Über die Reaktionsgeschwindigkeit bei der Inversion von Rohrzucker durch Säuren (on the reaction rate of the inversion of cane sugar by acids), *Z. Phys. Chem.*, *4*, 226–248.

Barclay, I. M., and J. A. V. Butler (1938), The entropy of solution, *Trans. Faraday Soc.*, *34*(2), 1445–1454.

Barrie, P. J. (2012a), The mathematical origins of the kinetic compensation effect. 2: The effect of systematic errors, *Phys. Chem. Chem. Phys.*, *14*(1), 327–336.

Barrie, P. J. (2012b), Reply to 'Comment on ''The mathematical origins of the kinetic compensation effect'' Parts 1 and 2' by A. Yelon, E. Sacher and W. Linert, Phys. Chem. Chem. Phys., 2012, 14, doi:10.1039/c2cp40618g, *Phys. Chem. Chem. Phys.*, *14*(22), 8235–8236.

Barrie, P. J. (2012c), The mathematical origins of the kinetic compensation effect. 1: The effect of random experimental errors, *Phys. Chem. Chem. Phys.*, *14*(1), 318–326.

Batyrmurzaev, A. S. (2003), Dehydration and diffusion of radiogenic argon in sericites from massif sulfide deposits of the Belokan-Shekin metallogenic zone, southern slope of the Greater Caucasus, Azerbaijan, *Geochem. Int.*, *41*(6), 559–564.

Bejina, F., and O. Jaoul (1997), Silicon diffusion in silicate minerals, *Earth Planet. Sci. Lett.*, *153*(3–4), 229–238.

Berenov, A. V., J. L. MacManus-Driscoll, and J. A. Kilner (2001), Observation of the compensation law during oxygen diffusion in perovskite materials, *Int. J. Inorg. Mater.*, *3*(8), 1109–1111.

Boisvert, G., L. J. Lewis, and A. Yelon (1995), Many-body nature of the Meyer-Neldel compensation law for diffusion, *Phys. Rev. Lett.*, *75*(3), 469–472.

Brady, J. B., and D. J. Cherniak (2010), Diffusion in minerals: An overview of published experimental diffusion data, in *Diffusion in Minerals and Melts*, edited by Y. X. Zhang and D. J. Cherniak, pp. 899–920, Mineralogical Society of America, Chantilly, USA, Reviews in Mineralogy & Geochemistry, vol. 72, doi:10.2138/rmg.2010.72.20.

Constable, F. H. (1925), The mechanism of catalytic decomposition, *Proc. R. Soc. London, Ser. A*, *108*(746), 355–378.

Cook, R. D. (1977), Detection of influential observation in linear-regression, *Technometrics*, *19*(1), 15–18.

Cremer, E., and G. M. Schwab (1929), A possible connection between activation heat and activity on contact catalyses, *Z. Phys. Chem.*, *144*(3/4), 243–243.

Demouchy, S. (2010), Diffusion of hydrogen in olivine grain boundaries and implications for the survival of water-rich zones in the Earth's mantle, *Earth Planet. Sci. Lett.*, *295*(1–2), 305–313.

Demouchy, S. (2012), Erratum to ''Diffusion of hydrogen in olivine grain boundaries and implications for the survival of water-rich zones in Earth's mantle'' [Earth Planet. Sci. Lett. 295 (2010) 305–313], *Earth Planet. Sci. Lett.*, *351*, 355–355.

Dohmen, R., and R. Milke (2010), Diffusion in polycrystalline materials: Grain boundaries, mathematical models, and experimental data, in *Diffusion in Minerals and Melts*, edited by Y. X. Zhang and D. J. Cherniak, 72, pp. 921–970, Mineralogical Society of America, Chantilly, USA, Reviews in Mineralogy & Geochemistry, vol. 72, doi:10.2138/rmg.2010.72.21.

Dunstan, D. J. (1998), The role of experimental error in Arrhenius plots: Self-diffusion in semiconductors, *Solid State Commun.*, *107*(4), 159–163.

Dyre, J. C. (1986), A phenomenological model for the Meyer-Neldel rule, *J. Phys. C Solid State Phys.*, *19*(28), 5655–5664.

Farver, J. R. (2010), Oxygen and hydrogen diffusion in minerals, in *Diffusion in Minerals and Melts*, edited by Y. X. Zhang and D. J. Cherniak, 72, pp. 447–507, Mineralogical Society of America Chantilly, USA, Reviews in Mineralogy & Geochemistry, vol. 72, doi:10.2138/rmg.2010.72.10.

Fasano, G., and R. Vio (1988), Fitting a straight line with errors on both coordinates, *Newslett. Working Group Mod. Astron. Methodol.*, *7*, 2–7.

Hanggi, P., P. Talkner, and M. Borkovec (1990), Reaction-rate theory—50 years after Kramers, *Rev. Mod. Phys.*, *62*(2), 251–341.

Hansen, P. C. (1992), Analysis of discrete ill-posed problems by means of the L-curve, *SIAM Rev.*, *34*(4), 561–580.

Hart, S. R. (1981), Diffusion compendation in natural silicates, *Geochim. Cosmochim. Acta*, *45*(3), 279–291.

Ingrin, J., and M. Blanchard (2006), Diffusion of hydrogen in minerals, in *Water in Nominally Anhydrous Minerals*, vol. 62, edited by H. Keppler and J. R. Smyth, pp. 291–320, Mineral. Soc. of Am., Washington, D. C.

Jaoul, O., and F. Bejina (2005), Empirical determination of diffusion coefficients and geospeedometry, *Geochim. Cosmochim. Acta*, *69*(4), 1027–1040.

Jaoul, O., and V. Sautter (1999), A new approach to geospeedometry based on the 'compensation law', *Phys. Earth Planet. Inter.*, *110*(1–2), 95–114.

Jones, A. G. (2014), Reconciling different equations for proton conduction using the Meyer-Neldel compensation rule, *Geochem. Geophys. Geosyst.*, *15*, 337–349, doi:10.1002/2013GC004911.

Jones, A. G., J. Fullea, R. L. Evans, and M. R. Muller (2012), Water in cratonic lithosphere: Calibrating laboratory-determined models of electrical conductivity of mantle minerals using geophysical and petrological observations, *Geochem. Geophys. Geosyst.*, *13*, Q06010, doi: 10.1029/2012GC004055.

Karato, S. I. (1990), The role of hydrogen in the electrical conductivity of the upper mantle, *Nature*, *347*(6290), 272–273.

Korolyuk, V. N., and G. G. Lepezin (2008), Analysis of experimental data on the diffusion coefficients of Fe, Mn, Mg, and Ca in garnets, *Russ. Geol. Geophys.*, *49*(8), 557–569.

Kreuer, K. D. (1999), Aspects of the formation and mobility of protonic charge carriers and the stability of perovskite-type oxides, *Solid State Ionics*, *125*(1–4), 285–302.

Libowitzky, E., and A. Beran (1995), OH defects in forsterite, *Phys. Chem. Miner.*, *22*(6), 387–392.

Linert, W., and A. Yelon (2013), Isokinetic relationships preface, *Monatshefte Chem.*, *144*(1), 1–2.

Lloyd, J., and J. A. Taylor (1994), On the temperature-dependence of soil respiration, *Funct. Ecol.*, *8*(3), 315–323.

Lubianiker, Y., and I. Balberg (1997), Two Meyer-Neldel rules in porous silicon, *Phys. Rev. Lett.*, *78*(12), 2433–2436.

Madamba, P. S., R. H. Driscoll, and K. A. Buckle (1996), The thin-layer drying characteristics of garlic slices, *J. Food Eng.*, *29*(1), 75–97.

Manche, E. P., and B. Carroll (1979), Compensation and the Smith-Topley effects, *Thermochim. Acta*, *31*(3), 387–390.

Mehta, N. (2010), Meyer-Neldel rule in chalcogenide glasses: Recent observations and their consequences, *Curr. Opin. Solid State Mater. Sci.*, *14*(5), 95–106.

Meyer, W., and H. Neldel (1937), Concerning the relationship between the energy constant epsilon and the quantum constant alpha in the conduction-temperature formula in oxydising semi-conductors, *Phys. Z.*, *38*, 1014–1019.

Padrón-Navarta, J. A., J. Hermann, and H. S. C. O'Neill (2014), Site-specific hydrogen diffusion rates in forsterite, *Earth Planet. Sci. Lett.*, *392*, 100–112.

Polissar, M. J. (1930), The kinetics, statics and energetics of the thermal reaction CH2I-CH2I=CH2=CH2+I-2 in carbon tetrachloride solutions, *J. Am. Chem. Soc.*, *52*, 956–969.

Polissar, M. J. (1932), The relation between the two constants of the arrhenius equation, *J. Am. Chem. Soc.*, *54*, 3105–3111.

Ratkowsky, D. A., J. Olley, T. A. McMeekin, and A. Ball (1982), Relationship between temperature and growth-rate of bacterial cultures, *J. Bacteriol.*, *149*(1), 1–5.

Rousseeuw, P. J. (1984), Least median of squares regression, *J. Am. Stat. Assoc.*, *79*(388), 871–880.

Schwab, G. M. (1929), A possible connection between activation heat and activity among contact catalysis Pi, *Z. Phys. Chem.*, *5*(6), 406–412.

Schwab, G. M. (1950), About the mechanism of contact catalysis, *Adv. Catal.*, *2*, 251–267.

Shimakawa, K., and M. Aniya (2013), Dynamics of atomic diffusion in condensed matter: Origin of the Meyer-Neldel compensation law, *Monatshefte Chem.*, *144*(1), 67–71.

Solis, C., and J. M. Serra (2011), Adjusting the conduction properties of $La_{0.995}Ca_{0.005}NbO_{(4-d)}$ by doping for proton conducting fuel cells electrode operation, *Solid State Ionics*, *190*(1), 38–45.

Sundvall, R., H. Skogby, and R. Stalder (2009), Hydrogen diffusion in synthetic Fe-free diopside, *Eur. J. Mineral.*, *21*(5), 963–970.

Widenhorn, R., A. Rest, and E. Bodegom (2002), The Meyer-Neldel rule for a property determined by two transport mechanisms, *J. Appl. Phys.*, *91*(10), 6524–6528.

Winchell, P. (1969), The compensation law for diffusion in silicates, *High Temp. Sci.*, *1*, 200–215.

Yelon, A., B. Movaghar, and H. M. Branz (1992), Origin and consequences of the compensation (Meyer-Neldel) law, *Phys. Rev. B*, *46*(19), 12,244–12,250.

Yelon, A., B. Movaghar, and R. S. Crandall (2006), Multi-excitation entropy: Its role in thermodynamics and kinetics, *Rep. Prog. Phys.*, *69*(4), 1145–1194.

Yelon, A., E. Sacher, and W. Linert (2012), Comment on "The mathematical origins of the kinetic compensation effect" Parts 1 and 2 by P. J. Barrie, Phys. Chem. Chem. Phys., 2012, 14, 318 and 327, *Phys. Chem. Chem. Phys.*, *14*(22), 8232–8234.

York, D. (1966), Least-squares fitting of a straight line, *Can. J. Phys.*, *44*(5), 1079–1086.

Zawadzki, J., and S. Bretsznajder (1935), Concerning the temperature increment of the rate of reaction in reactions of the type A(solid)= B-solid+C-gas, *Z. Elektr. Angew. Phys. Chem.*, *41*, 215–223.

Zhang, B. H., X. P. Wu, and R. L. Zhou (2011), Calculation of oxygen self-diffusion coefficients in Mg_2SiO_4 polymorphs and $MgSiO_3$ perovskite based on the compensation law, *Solid State Ionics*, *186*(1), 20–28.

Zhao, Z. F., and Y. F. Zheng (2007), Diffusion compensation for argon, hydrogen, lead, and strontium in minerals: Empirical relationships to crystal chemistry, *Am. Miner.*, *92*(2–3), 289–308.

Zheng, Y. F., and B. Fu (1998), Estimation of oxygen diffusivity from anion porosity in minerals, *Geochem. J.*, *32*(2), 71–89.